ELSEVIER

European Journal of Pharmacology 387 (2000) 179–188

ejp

www.elsevier.nl/locate/ejphar

Imaging extrastriatal dopamine D_2 receptor occupancy by endogenous dopamine in healthy humans

Masahiro Fujita [a,*], N. Paul L.G. Verhoeff [a], Andrea Varrone [a], Sami S. Zoghbi [c], Ronald M. Baldwin [a], Peter A. Jatlow [b], George M. Anderson [a], John P. Seibyl [a,c], Robert B. Innis [a,d]

[a] *Department of Psychiatry, Yale University, VA Connecticut, West Haven, CT, USA*
[b] *Department of Laboratory Medicine, Yale University, New Haven, CT, USA*
[c] *Department of Diagnostic Radiology, Yale University, VA Connecticut, West Haven, CT, USA*
[d] *Department of Pharmacology, Yale University, New Haven, CT, USA*

Received 29 July 1999; received in revised form 11 November 1999; accepted 16 November 1999

Abstract

The effect of endogenous dopamine on in vivo measurement of dopamine D_2 receptors in extrastriatal regions (thalamus and temporal cortex) was evaluated with single photon emission computed tomography and the high affinity ligand [^{123}I]epidepride by comparing the binding potential before and after acute dopamine depletion. Dopamine depletion was achieved by per-oral administration of 5.5 g/70 kg body weight α-methyl-*para*-tyrosine given in 37 h. The α-methyl-*para*-tyrosine treatment increased the binding potential significantly in the temporal cortex ($13 \pm 15\%$, $P = 0.036$) but not in the thalamus ($2 \pm 9\%$). The increase of the binding potential in the temporal cortex correlated strongly with the increase of dysphoric mood evaluated by the Positive and Negative Symptom Scale (PANSS) ($\rho = 0.88$, $P = 0.004$). These results imply that [^{123}I]epidepride, coupled with acute dopamine depletion might provide estimates of synaptic dopamine concentration.

Keywords: Dopamine; Dopamine D_2 receptor, extrastriatal; [^{123}I]Epidepride; SPECT (Single photon emission computed tomography); α-Methyl-*para*-tyrosine; Schizophrenia; Binding, in vivo

1. Introduction

The dopamine system in the brain is involved with major psychiatric disorders such as schizophrenia and mood disorders. The ''classical'' dopaminergic hypothesis of schizophrenia proposed that hyperactivity of dopamine transmission is responsible for the symptoms of the disorder (Seeman and Lee, 1975; Creese et al., 1976), but still lacks definitive experimental validation (for reviews see (Reynolds, 1989; Davis et al., 1991)) and must be modified to account for diversity and complexity of dopamine transmission in cortical and subcortical regions of the brain. Two recent reformulations of the dopamine hypothesis emphasized an imbalance between cortical and subcortical systems (Weinberger, 1987; Davis et al., 1991) and between baseline tonic and reactive phasic dopamine activity (Grace, 1993). According to the first formulation, negative symptoms of schizophrenia are related to decreased dopamine function in the cortex, whereas positive symptoms are associated with increased transmission in subcortical/mesolimbic dopamine pathways. According to the second formulation, low basal levels of synaptic dopamine predispose to excessive phasic or burst release of dopamine. In both formulations, negative symptoms of schizophrenia are associated with low dopamine function and positive symptoms with excessive dopamine transmission.

The binding of neuroreceptor ligands is sensitive to competition with endogenous neurotransmitter and may be used to assess both classical and revised dopamine theories of schizophrenia. Endogenous dopamine levels have re-

* Corresponding author. Department of Psychiatry, Yale University School of Medicine, VA Connecticut/116A2, 950 Campbell Avenue, West Haven, CT 06516, USA. Tel.: +1-203-932-5711 ext. 3590; fax: +1-203-937-3897.

E-mail address: masahiro.fujita@yale.edu (M. Fujita)

0014-2999/00/$ - see front matter
PII: S0014-2999(99)00817-1

cently been estimated with positron emission tomography (PET) using dopamine D_2 receptor ligands such as [^{11}C]raclopride (Volkow et al., 1994) and [^{18}F]*N*-methylspiroperidol (Dewey et al., 1991) and with single photon emission computed tomography (SPECT) using [^{123}I](*S*)-(−)-3-iodo-2-hydroxy-6-methoxy-*N*-[(1-ethyl-2-pyrrolidinyl)methyl]benzamide ([^{123}I]IBZM) (Innis et al., 1992; Laruelle et al., 1996; Laruelle et al., 1997). Two types of dopamine release have been measured, stimulant-induced release and baseline tonic release. The former can be estimated by comparing radiotracer binding (i.e., binding potential) at baseline and after amphetamine or methylphenidate challenges (Dewey et al., 1991; Innis et al., 1992; Volkow et al., 1994; Laruelle et al., 1996). The latter type of dopamine release can be estimated by comparing the binding potential at baseline and after a rapid dopamine depletion induced by the tyrosine hydroxylase inhibitor α-methyl-*para*-tyrosine (Laruelle et al., 1997). These studies have been confined to the striatum because of insufficient in vivo signal to noise ratio of the radiolabeled ligands. Since recent hypotheses of schizophrenia indicated an imbalance between cortical and subcortical dopamine systems (Weinberger, 1987; Davis et al., 1991) and an imbalance also in synaptic dopamine levels (Grace, 1993), measurement of dopamine levels in extrastriatal regions would help understand the pathology of this disorder. High-affinity ligands have recently been developed to study extrastriatal dopamine D_2 receptors with SPECT ([^{123}I]epidepride (Kessler et al., 1992)) and PET ([^{18}F]fallypride (Mukherjee et al., 1995; Rieck et al., 1997) and [^{11}C] or [^{76}Br] (*S*)-*N*-((1-ethyl-2-pyrrolidinyl)methyl)-5-bromo-2,3-dimethoxybenzamide (FLB 457) (Farde et al., 1997; Delforge et al., 1999)). We have developed and validated a method for quantification of extrastriatal dopamine D_2 receptors using [^{123}I]epidepride (Fujita et al., 1999; Ichise et al., 1999; Varrone et al., in press).

The purposes of the present investigation were to study (1) the influence of dopamine depletion on the binding potential of [^{123}I]epidepride in the thalamus and the lateral temporal cortex (subsequently referred to simply as the temporal cortex) where this tracer shows measurable specific binding, (2) regional difference in the changes of the binding potential, and (3) correlation between the changes of the binding potential and mood and behavior in healthy human subjects. For each subject, the binding potential at two baseline scans was compared to that after dopamine depletion achieved with oral administration of α-methyl-*para*-tyrosine (5.5 g/70 kg body weight in 37 h).

2. Materials and methods

2.1. Human subjects

The study was approved by the Yale institutional review board. All subjects gave written informed consent after complete explanation of the risks and possible consequences of the study. The absence of medical, neurological and psychiatric history (including alcohol and drug abuse) was assessed by history, physical examination, routine blood and urine tests, urine toxicology and electrocardiogram. Ten healthy subjects (4 males and 6 females; ages: 28.3 ± 9.6, with these and subsequent values expressed as mean ± S.D.) enrolled in the study and eight completed all three SPECT studies. Two subjects were withdrawn from the study, before the start of [^{123}I]epidepride infusion, on days 1 and 2 of α-methyl-*para*-tyrosine administration due to its side effects (akathisia and a significant increase of anxiety, respectively).

2.2. Depletion regimen and clinical monitoring

The subjects had three SPECT studies, two baseline scans (scans 1 and 2) and one with α-methyl-*para*-tyrosine administration (scan 3). These three scans were performed within 18.0 ± 8.7 days. Dopamine depletion was induced by oral administration of α-methyl-*para*-tyrosine, 5.5 g/70 kg body weight for 37 h. The subjects were hospitalized from 8 a.m. on the first day of α-methyl-*para*-tyrosine administration (day 1) to 8 a.m. on the day after scan 3 (day 3). On day 1, a total dose of 3 g/70 kg was given at 8 a.m., 1 p.m., 6 p.m. and 11 p.m. To minimize fluctuations of dopamine levels on day 2, which might differentially influence the binding of [^{123}I]epidepride in high and low density regions, α-methyl-*para*-tyrosine was administered more frequently, with a total dose of 2.5 g/70 kg given in 8 doses (every 2 h from 7 a.m. to 9 p.m.). On both day 1 and 2, doses were divided as evenly as possible. To prevent the formation of α-methyl-*para*-tyrosine crystals in the urine, subjects were instructed to drink at least 4 l of fluids on the day before day 1. During α-methyl-*para*-tyrosine administration, 0.45% saline was infused intravenously at a rate of 167 ml/h (4 l/24 h) through a computer-controlled pump (Abbott/Shaw LifeCare® Pump Model 4, Abbott Laboratories, North Chicago, IL 60064, USA).

The effects of α-methyl-*para*-tyrosine were evaluated with the Positive and Negative Symptom Scale (PANSS) interview and the Extrapyramidal Symptom Rating Scale (ESRS) (Chouinard et al., 1980). The PANSS scores were evaluated with five clinical dimensions (negative, positive, activation, dysphoric mood, and autistic preoccupation) recently evaluated in approximately 1200 patients (White et al., 1997). These evaluations were done during scans 1 and 2 and on day 1–3 of α-methyl-*para*-tyrosine administration. On day 2, the evaluations were done during the SPECT study and the PANSS was obtained when the subjects showed the largest scores. Weighted total scores were obtained in the five clinical dimensions (negative, positive, activation, dysphoric and autistic preoccupation) proposed by the PANSS Study Group (White et al., 1997). Urine samples were collected at 7 a.m. on days 2 and 3 to examine the presence of α-methyl-*para*-tyrosine crystals.

2.3. Radiolabeling

[^{123}I]Epidepride was prepared by iododestannylation from *N*-[(1-ethyl-2-pyrrolidinyl)-methyl]-2,3-dimethoxy-5-(tributylstannyl)benzamide as previously described (Baldwin et al., 1994). [^{123}I]Epidepride was obtained in radiochemical yield of $73.4 \pm 12.7\%$, $n = 24$, radiochemical purity of $98.0 \pm 1.5\%$, and a specific activity of $> 185{,}000$ GBq/mmol (> 5000 Ci/mmol), based on the limit of detection for epidepride).

2.4. Scan protocol

[^{123}I]Epidepride was infused continuously for 9 h, which provided equilibrium measurements in extrastriatal regions but not in the striatum. A much longer infusion, approximately 24 h, is required for the tracer to achieve equilibrium receptor binding levels in the striatum (Fujita et al., 1999). An advantage of this shorter, 9 h, protocol is better counting statistics in low density temporal cortex because of less decay of the radionuclide ^{123}I ($T_{1/2}$ 13.2 h) and lower bolus/infusion ratio (Varrone et al., in press).

Subjects had an intravenous infusion of 0.45% saline at a rate of 167 ml/h (4 l/24 h) in all three scans to make physiological conditions consistent. [^{123}I]Epidepride was administered with a total dose of 314 ± 13 MBq (bolus: 142 ± 6.5 MBq and constant infusion: 172 ± 6.7 MBq), bolus to infusion ratio of 6.00 ± 0.03 h, and duration of 8.82 ± 0.08 h (baseline studies) and 8.78 ± 0.08 h (during α-methyl-*para*-tyrosine administration). SPECT studies were performed with a three-headed camera (PRISM 3000 XP, Picker, Cleveland, OH, USA) equipped with low energy-high resolution (LEHR) fanbeams collimators. To check the quality of equilibrium during infusion of [^{123}I]epidepride, multiple images (15–48 min data acquisition) and blood samples were acquired. Twelve and eleven images were acquired during scans 1–2 and 3, respectively. Six blood samples (10 ml each) were obtained from 3 h post bolus to the end of the infusion. Due to every 2 h administration of α-methyl-*para*-tyrosine, the number of image acquisitions was smaller during scan 3. In scan 3, the infusion of the tracer was started at 1:45 p.m. to make the intervals between scans and α-methyl-*para*-tyrosine doses consistent between studies.

To identify brain regions, magnetic resonance imaging (MRI) scans of 3 mm contiguous slices were obtained with a 1.5 T GE Signa device. Axial images were acquired with a spoiled GRASS (gradient recall acquisition in the steady state) sequence with time-to-recovery (TR) = 25 ms, time-to-echo (TE) = 5 ms, number of excitation = 1, matrix = 256×256, field of view = 24 cm.

2.5. Plasma [^{123}I]epidepride metabolite analysis

Concentrations of parent and metabolites in the plasma were determined by extraction with ethyl acetate followed by high performance liquid chromatography (HPLC) of the dried extract (Waters Novapak C18, methanol/water/triethylamine, 75/25/0.1, 1.0 ml/min) as previously described for [^{123}I]iomazenil (Zoghbi et al., 1992).

2.6. Homovanillic acid (HVA) and 3-methoxy-4-hydroxyphenylethyleneglycol (MHPG) plasma analysis

Plasma levels of HVA and a norepinephrine metabolite MHPG were measured to assess the effect of α-methyl-*para*-tyrosine on dopamine synthesis. Blood samples were obtained at 1 p.m., 5 p.m. and 9 p.m. in scans 1 and 3.

For the measurement of HVA levels, an internal standard (iso-homovanillic acid, 20 μL of 0.1 ng/ml; final concentration 33.3 ng/ml) was added to 60 μl of plasma ultrafiltrate prepared by centrifuging 250 μl of plasma for 20 min at $6400 \times$ g (0–4°C) in a disposable Ultrafree-MC ultrafiltration device (#UFC3LGC25; Millipore, Bedford, MA, USA). Levels of HVA were determined using a modification of a previously reported method for the determination of cerebrospinal fluid HVA (Anderson et al., 1979). After direct injection of 10–20 μl of ultrafiltrate, the compounds were separated using a mobile phase of 85% pH 4.00 1.0% acetic acid containing 25 mg/l of EDTA/10% methanol/5% acetonitrile (1 ml/min), and a 15×0.46 cm Microsorb-MV C18 column (Varian, Walnut Creek, CA, USA). Coulometric detection was performed using a Coulochem II detector (ESA, Chelmsford, MA, USA) in the 3-electrode redox mode. After initial oxidation at +500 mV, a reductive screening electrode was set at −100 mV, followed by the analytical reductive working electrode set at a potential of −350 mV. A detection limit of 5 pg was obtained for HVA. Recovery of HVA and iso-HVA added to plasma before or after ultrafiltration was greater than 95% and the method was highly correlated ($r = 0.98$, $n = 16$) with a gas chromatographic-mass spectrometric method. A pooled quality assessment sample was determined with a coefficient of variation of 5.1% ($n = 6$).

Plasma concentrations of MHPG were determined by gas chromatography-mass spectrometry following ethyl acetate extraction and preparation of the acetyl/trifluoracetyl derivative (Elsworth et al., 1983). Tri-deuterated MHPG was used as the internal standard (200 ng/ml); a pooled quality assessment sample was determined with a day-to-day coefficient of variation of 9.9%.

2.7. α-Methyl-para-tyrosine plasma analysis

Plasma levels of α-methyl-*para*-tyrosine were measured on each subject during the third SPECT study. Blood samples were obtained just before the α-methyl-*para*-tyrosine administration at 1 p.m., 5 p.m. and 9 p.m. in scan 3. Plasma α-methyl-*para*-tyrosine concentrations were measured by reversed-phase HPLC with fluorescence detection as described previously (Laruelle et al., 1997).

2.8. Image analysis

SPECT images of all three scans were coregistered with each other using either the AIR (Automatic Image Registration) (Woods et al., 1993) module in MEDx™ 2.1 (Multimodality Radiological Image Processing, Sensor System, Sterling, VA, USA) or the ''coregister'' function in SPM96 (Statistical Parametric Mapping version '96) (Friston et al., 1995). Non-uniform attenuation correction was done using an attenuation map created with a ^{57}Co line source (Rajeevan et al., 1998). MRI scans were coregistered to SPECT images using either ''coregister'' function in SPM96 or the AIR module in MEDx™ 2.1. One of the two methodologies of coregistration was selected based on visual evaluation of the results.

Data of volumes of interest were obtained from the thalamus, temporal cortex (including superior, middle and inferior gyri), cerebellum, caudate and putamen. The data of caudate and putamen were used to estimate the influence of scatter from these regions (see Section 4). The volume of interest for the thalamus was elliptical in shape and placed on a high uptake region in SPECT images. Although an in vitro study showed heterogeneous binding of the tracer in the thalamus (Hall et al., 1996), the resolution of SPECT is not enough to show this heterogeneous distribution. The volumes of interest for the temporal cortex, cerebellum, caudate and putamen were placed on four slices (3.56 mm thickness) of the coregistered MRI for individual subject. The sizes of the volumes of interest (ml) were: thalamus: 5.37, temporal cortex: 26.3 ± 2.3, cerebellum: 22.5 ± 2.6, caudate: 4.66, and putamen: 7.53. A fixed size of volume of interest was used for the thalamus, caudate and the putamen in all subjects. The data of caudate and putamen were averaged and reported as a single value for the striatum.

V_3' (= (specific binding/total (free + protein bound) tracer in plasma) at equilibrium) (Abi-Dargham et al., 1995) was used because the reliability of this outcome measure was the best among V_3', V_3 (= binding potential = specific binding/free tracer in plasma), and R_T (specific/non-displaceable tissue ratio at equilibrium) in a test retest study (Varrone et al., in press). The cerebellum was used as a receptor-free region to calculate specific binding. V_3' was obtained by averaging those time points at which % change/h of total regional activity in the thalamus was less than 2% (see Section 3). For those studies in which % change/h was greater than 2% (13 scans), only the last point was used for deriving outcome measures. This strategy was applied because it provided measures with slightly better reproducibility in two baseline scans than the one using only the last point.

2.9. Statistical analyses

Mean V_3' values of scans 1 and 2 were used as baseline because they best represented true baseline values without errors in the measurement. α-methyl-*para*-tyrosine effects on the PANSS, plasma HVA and MHPG levels, and scan measurements were assessed by the Friedman one-way analysis of variance (ANOVA), repeated-measures multivariate analysis of variance (MANOVA), and the Wilcoxon signed ranks test, respectively. The differences between the changes of HVA and MHPG and between those of V_3' in the thalamus and the temporal cortex were tested by the Wilcoxon signed ranks test. Correlations were analyzed using Spearman rank correlation. Significant differences from zero were evaluated by one sample *t*-tests. All tests were performed with the software SPSS 9.0 for Windows (SPSS, Chicago, IL, USA). All tests were two-tailed and a probability value of 0.05 was used as the significance level.

3. Results

3.1. Clinical effects of α-methyl-para-tyrosine

α-Methyl-*para*-tyrosine effects on mood were scored by the PANSS (Table 1). None of the five clinical dimensions showed a significant change by the α-methyl-*para*-tyrosine administration after correction for multiple comparison (in this case, comparisons for the five clusters). However, α-methyl-*para*-tyrosine showed relatively large effects on dysphoric mood and autistic preoccupation ($P < 0.01$ without correction for multiple comparisons). In fact, two subjects were withdrawn from the study due to significant increases in dysphoric mood states (anxiety and tension). As shown in a large S.D. in the scores under α-methyl-*para*-tyrosine administration, there was a large intersubject variability in the change of the dysphoric mood cluster.

Lorazepam 1 mg, p.o. was given for akathisia in six subjects at 5.0 ± 2.1 h of [^{123}I]epidepride infusion. This drug was given only once in these subjects. Two of the eight subjects showed acute dystonic reactions on the back and the neck during the scanning sessions. In these cases, 100 mg and 75 mg diphenhydramine was orally adminis-

Table 1
Effect of α-methyl-*para*-tyrosine administration on PANSS scores

PANSS clusters[a]	Baseline	α-Methyl--*para*-tyrosine admin.	Day after α-methyl-*para*-tyrosine	P[b]
Negative	5.8 ± 0.8	6.8 ± 1.7	5.6 ± 0.7	> 0.1
Positive	2.8 ± 0.2	3.0 ± 0.6	2.7 ± 0.2	> 0.1
Activation	2.7 ± 0.1	3.0 ± 0.5	2.7 ± 0.0	> 0.1
Dysphoric	3.0 ± 0.8	4.9 ± 2.9	2.6 ± 0.0	0.06
Autistic Preoccupation	3.5 ± 0.2	3.8 ± 0.5	3.4 ± 0.2	0.04

[a] The score of each PANSS cluster is the summation of each item multiplied by the factor loading (White et al., 1997).
[b] Without correction for multiple comparison.

Table 2
Effect of α-methyl-*para*-tyrosine administration on plasma homovanillic acid
α-methyl-*para*-tyrosine and HVA were measured at −1, 3, and 7 h of [^{123}I]epidepride infusion.
Change in HVA was calculated as 100 × (α-methyl-*para*-tyrosine admin. − baseline)/baseline.

Subject #	Age/sex	α-methyl-*para*-tyrosine (μg/ml)	HVA (ng/ml)		Change HVA (%)
			Baseline	α-methyl-*para*-tyrosine admin.	
1	33/M	22.7 ± 3.2	5.6 ± 0.8	1.5 ± 0.4	−74
2	25/F	20.7 ± 2.3	10.9 ± 1.0	2.6 ± 0.4	−76
3	19/M	15.3 ± 1.5	5.9 ± 1.4	2.0 ± 0.3	−65
4	19/F	20.0 ± 1.0	5.5 ± 1.1	2.2 ± 0.5	−60
5	19/M	15.3 ± 0.6	5.7 ± 1.1	2.2 ± 0.1	−62
6	21/F	18.7 ± 2.1	8.9 ± 1.5	3.8 ± 1.2	−57
7	46/F	40.3 ± 2.1	9.8 ± 3.6	2.4 ± 0.1	−76
8	34/F	18.3 ± 1.5	5.4 ± 0.3	3.0 ± 1.0	−44
Mean ± S.D.	27 ± 10	21.4 ± 8.0	7.2 ± 2.3	2.5 ± 0.7	−64 ± 11

tered, respectively, with complete response. The other six subjects showed mild or no extrapyramidal symptoms. Among them, the rating of Parkinsonism in the ESRS showed a borderline level in three and no apparent abnormality in three subjects. Lorazepam was given for akathisia before the rating in one of the latter three subjects. At 8 a.m. on day 3, two subjects still showed a borderline Parkinsonism and the other six subjects did not show any abnormalities.

3.2. Plasma α-methyl-para-tyrosine

The average α-methyl-*para*-tyrosine plasma concentration was 21.4 ± 8.0 μg/ml (Table 2). The oldest (46 years old) female subject showed a high level, presumably due to age-related decline of the clearance of this drug. This subject also showed the second lowest clearance of [^{123}I]epidepride (31.5 l/h), in comparison to the group mean 42.6 ± 13.9 l/h.

3.3. Plasma HVA and MHPG

α-methyl-*para*-tyrosine significantly decreased plasma HVA by 64 ± 11% (repeated measures MANOVA, $P = 0.01$, range from 44% to 76%, Table 2) and plasma MHPG by 51 ± 11% ($P = 0.005$, range from 31% to 67%). Plasma HVA and MHPG were not correlated either at baseline or after α-methyl-*para*-tyrosine administration. There was a significant difference in the decrease of HVA and MHPG ($P = 0.01$).

3.4. SPECT results

The quality of equilibrium state was assessed by measuring the changes of activities over time in plasma total parent, the thalamus, the temporal cortex and the cerebellum (Table 3). Little change was observed in plasma total parent, the temporal cortex and the cerebellum in all three scans, whereas a small increase was detected in the thalamus where receptor density is greater. Only the change in the thalamus at baseline scans (scans 1 and 2) was significantly different from zero, while there was no significant difference between the changes at scans 1–2 and 3 (α-methyl-*para*-tyrosine administration) in the thalamus ($P = 0.48$). Therefore, at scans 1 and 2, the measurement might have been done slightly before achieving equilibrium in the thalamus and V_3' in this region might have been underestimated. All other measurements were done under appropriate equilibrium conditions.

Table 3
Changes of activities over time (% change/h)
The numbers in parentheses are 95% confidence intervals.
The changes were measured after 5.3 ± 0.1 h and 5.2 ± 0.1 h for plasma and brain data, respectively, in baseline scans and after 4.8 ± 0.2 h for all data in the scans under α − methyl-*para*-tyrosine administration.

	Thalamus	Temporal cortex	Cerebellum	Parent in plasma
Baseline	2.5 ± 1.0 (+1.6–+3.3)	0.9 ± 1.5 (−0.4–+2.1)	0.7 ± 1.1 (−0.3–+1.6)	0.1 ± 2.0 (−1.6–+1.7)
α-methyl-*para*-tyrosine admin.	1.7 ± 2.8 (−0.7–+4.0)	0.2 ± 1.5 (−1.1–+1.5)	−0.6 ± 2.3 (−2.4–+1.3)	−0.1 ± 1.9 (−1.7–+1.4)

Table 4
Effect of α-methyl-*para*-tyrosine administration on [^{123}I]epidepride binding potential (V_3')
Numbers in parentheses: results in two baseline scans.

Subject #	Thalamus			Temporal cortex		
	Baseline	α-methyl-*para*-tyrosine admin.	Change (%)	Baseline	α-methyl-*para*-tyrosine admin.	Change (%)
1	12.7 (14.0, 11.4)	13.9	9.6	4.8 (5.5, 4.2)	5.3	10.5
2	16.3 (19.0, 13.6)	15.7	−4.1	5.2 (5.8, 4.7)	7.6	44.7
3	17.0 (17.6, 16.3)	18.0	6.0	5.7 (5.6, 5.8)	6.8	19.1
4	14.2 (14.0, 14.4)	16.7	17.2	7.4 (7.2, 7.7)	8.7	17.0
5	15.5 (15.7, 15.3)	14.8	−4.2	6.2 (6.0, 6.3)	6.3	1.5
6	20.5 (21.2, 19.8)	20.9	1.8	7.4 (7.9, 6.9)	8.1	9.4
7	9.5 (8.9, 10.1)	9.2	−3.2	2.2 (2.2, 2.2)	2.3	5.5
8	17.5 (18.9, 16.1)	16.0	−8.6	7.3 (8.1, 6.5)	7.1	−2.6
Mean ± S.D.	15.4 ± 3.4	15.6 ± 3.4	1.8 ± 8.6	5.8 ± 1.8	6.5 ± 2.0	13.1 ± 14.7[a]

[a] $P = 0.036$. Change in binding potential was calculated as $100 \times$ (α-methyl-*para*-tyrosine admin. − baseline)/baseline.

Table 4 shows the changes in V_3' by the α-methyl-*para*-tyrosine administration. V_3' in the thalamus showed only a small and non-significant increase of 1.8 ± 8.6%. V_3' in the temporal cortex showed a significant increase of 13.1 ± 14.7% ($P = 0.036$). In both of these regions, there was a large inter-subject variability of the changes ranging from −8.6 to +17.2% in the thalamus and from −2.6 to +44.7% in the temporal cortex. In the latter region, only one subject showed a small decrease. The increase in V_3' was significantly greater in the temporal cortex than in the thalamus ($P = 0.017$).

Correlation analyses were performed between the significant increase of V_3' in the temporal cortex and other results. Among the five clusters of the PANSS items, only the dysphoric mood cluster showed a significant correlation (Fig. 1). This correlation was strong, with Spearman's $\rho = 0.88$ and $P = 0.004$ (by Bonferroni's correction for the comparisons for the five clusters, significance level is $0.05/5 = 0.01$). The other four clusters, including autistic preoccupation, which showed a small non-significant effect of α-methyl-*para*-tyrosine administration (Table 1), did not show any significant correlation with the increase of V_3' in the temporal cortex ($0.19 < \rho < 0.37$, $0.37 < P < 0.65$). There was no correlation between the increase in V_3' and the decrease in plasma HVA ($\rho = 0.55$, $P = 0.16$) or MHPG ($P = 0.82$), which indicated that synaptic dopamine in the temporal cortex contributed only to a small part of plasma HVA. There was no correlation between baseline V_3' and the α-methyl-*para*-tyrosine-induced increase in V_3' ($P = 0.81$) and between the increase in V_3' and plasma α-methyl-*para*-tyrosine levels ($P = 0.67$).

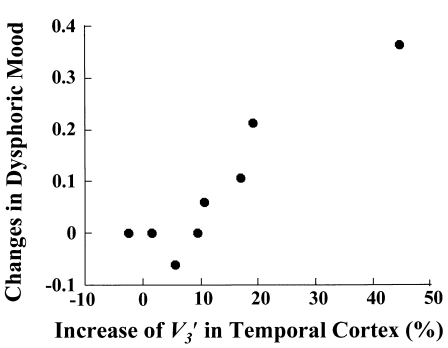

Fig. 1. Relationship between α-methyl-*para*-tyrosine-induced increase in [^{123}I]epidepride V_3' in the temporal cortex and the dysphoric mood cluster measured by the PANSS.

4. Discussion

This study showed that acute dopamine depletion by α-methyl-*para*-tyrosine administration induced a significant increase (13.1 ± 14.7%) of [^{123}I]epidepride V_3' in the temporal cortex but not in the thalamus. This increase in the temporal cortex showed a strong correlation with only dysphoric mood cluster (Spearman's $\rho = 0.88$ and $P = 0.004$) among the five clusters of the PANSS items.

These results suggested that V_3' in the temporal cortex was affected by endogenous dopamine levels while V_3' in the thalamus was not. However, several limitations must be taken into account: (1) The increase in [^{123}I]epidepride V_3' after α-methyl-*para*-tyrosine administration might have reflected receptor upregulation rather than removal of endogenous dopamine. However, previous animal studies indicated that dopamine depletion for two days did not cause receptor upregulation. In mice, while reserpine administration induced about a 100% increase of in vivo binding of [^{3}H]raclopride 3 days later, B_{max} measured in vitro showed no change (increase was less than 0.5%) (Ross and Jackson, 1989). In rats dopamine depletion induced by 6-hydroxydopamine (Narang and Wamsley, 1995) or α-methyl-*para*-tyrosine (Laruelle et al., 1997) did not cause a significant receptor upregulation in one week or two days, respectively. In Cynomolgus monkeys, dopamine depletion induced by reserpine administration did not change B_{max} measured in vivo using [^{11}C]raclopride PET (Ginovart et al., 1997). Although these results cannot be fully extrapolated to human extrastriatal regions, receptor upregulation does not seem to play a major role in the effects of α-methyl-*para*-tyrosine detected in this study.

(2) The activities in the thalamus at scans 1 and 2 showed a trend of a slight increase. However, the changes in the thalamus at scans 1–2 and 3 were not significantly different. Therefore, although there is a possibility of a slight underestimation of V_3' at baseline in the thalamus, the error should have been minimal. In addition, this underestimation would have caused an overestimation of the increase of V_3' in the thalamus by α-methyl-*para*-tyrosine administration, which was still not significant.

(3) One controversial point in this study is the administration of lorazepam for akathisia. Most subjects would have withdrawn from the protocol without medication treatment. It may cause changes in dopamine levels through GABA-dopamine interaction (Dewey et al., 1992). To examine this possibility, equilibrium ratio of specific:non-displaceable (R_T) in the temporal cortex was compared before (mean of two scans just before the administration) and 1.1 ± 0.3 h after the administration. This comparison was justified because an equilibrium was achieved early in this low density region. There was no change in R_T ($+0.6 \pm 3.5\%$). This result may be interpreted that lorazepam did not show effects through GABA-dopamine interaction because dopamine had already been depleted before the administration. (4) One weak point of this SPECT study was that no scatter correction was performed. In this 9-h infusion protocol, an equilibrium was not achieved in the striatum, and the activity in this region continued to increase (Varrone et al., in press). Measurement in extrastriatal regions might have been influenced by the high uptake in this region. To estimate the influence of the scatter from the striatum and limited resolution of the camera, an anthropomorphic phantom study (Radiologic Support Devices, Long Beach, CA, USA) was performed in which the striatum was filled with a uniform solution of ^{123}I and the remainder of the brain was filled with water (Varrone et al., in press). From this phantom study, the influence of high activity in the striatum was estimated to be 17–30% of the counts in the thalamus and 4–7% in the temporal cortex. Therefore, measurement in extrastriatal regions has been influenced by the scatter from the striatum, with more significant effects in the thalamus, which is closer to the striatum, and the reliability of the results in the two extrastriatal regions was different. A first-order correction was performed for the influence from the high activity in the striatum by subtracting fractions of striatal counts obtained in the phantom (7.5% of striatal counts in the thalamus and 0.92% in the temporal cortex) from the counts in the extrastriatal regions. Although a scatter correction algorithm (Iida et al., 1998) is required for more accurate quantification, this first order compensation indicated that scatter correction would not significantly change the results of this study. The increase of V_3' in the temporal cortex showed only a minor change after correction (from $13.1 \pm 14.7\%$, $P = 0.036$ to $13.8 \pm 14.9\%$, $P = 0.036$) and the increase in the thalamus after the correction ($4.2 \pm 9.3\%$, $P = 0.33$) was still much smaller than the increase in the temporal cortex and was not statistically significant. Therefore, all of these considerations indicate that a reduction in endogenous dopamine is the major factor to increase V_3' in the temporal cortex; the influence of dopamine depletion appeared to be much smaller in the thalamus.

Some imaging investigators believe that dopamine levels will only influence binding of low affinity tracers, since dopamine would not be able to compete with a high-affinity tracer (Seeman et al., 1989). In fact, low affinity ligands such as [^{11}C]raclopride ($K_d \approx 1$ nM; K_d of [^{123}I]epidepride ≈ 0.03 nM) (Dewey et al., 1992; Volkow et al., 1994; Breier et al., 1997; Endres et al., 1997) and [^{123}I]IBZM ($K_d \approx 0.4$ nM) (Innis et al., 1992; Laruelle et al., 1996, 1997) have been widely used to estimate endogenous dopamine levels. Amphetamine-induced dopamine release did not displace binding of [^{123}I]epidepride (Kessler et al., 1993; Al-Tikriti et al., 1994). However, time-varying changes of both [^{123}I]epidepride and dopamine levels should be taken into account to interpret the results of these studies in which [^{123}I]epidepride was administered as a bolus followed by a bolus injection of amphetamine near or after the time of peak uptake. In this experimental design, displacement of a radiolabeled tracer should mainly be affected by its in vivo off rate (k_4). In fact, the k_4 of [^{123}I]epidepride (0.003 min^{-1} in the striatum) (Fujita et al., 1999) was much smaller than that of [^{11}C]raclopride (0.06–0.13 min^{-1} in the striatum) (Farde et al., 1989; Ito et al., 1998). That is, under non-equilibrium conditions, the k_4 of [^{123}I]epidepride may be too slow to monitor the much more rapidly changing dopamine levels induced by amphetamine.

In the present study, [^{123}I]epidepride V_3' was measured under equilibrium condition; i.e., the levels of both brain and plasma parent activities were stable for about 3 h. In the presence of a competitive inhibitor such as endogenous dopamine, both the Michaelis–Menten and Cheng–Prusoff equations would predict that % receptor occupancy by the displacing agent would be independent of the affinity of the radioligand. In contrast to rapidly changing dopamine levels induced by amphetamine, the depletion induced by frequently administered α-methyl-*para*-tyrosine should maintain fairly stable (and decreased) levels of synaptic dopamine. Thus, the current paradigm was designed to achieve equilibrium receptor binding conditions for both the radioligand (i.e., [^{123}I]epidepride) and the displacing agent (i.e., dopamine). Consistent with both theory and validated in vitro receptor binding practice, the current paper demonstrates in vivo occupancy of dopamine D_2 receptors can be estimated using even a high-affinity radiotracer.

Although there are several confounding factors as discussed above, their influence appears to be minor and V_3' in the temporal cortex was truly increased by the depletion of endogenous dopamine whereas V_3' in the thalamus was not. The change in the temporal cortex (13%) was smaller

than the change in the striatum measured with [^{123}I]IBZM (28%) (Laruelle et al., 1997) but comparable to the change measured with the same tracer in a second report (11%) (Abi-Dargham et al., 1999). The results of the present study indicate that the influence of dopamine depletion on the binding of dopamine D_2 receptor ligands is greater in the temporal cortex than in the thalamus. The most straightforward interpretation is that receptor occupancy by dopamine at baseline is greater in the temporal cortex than that in the thalamus. However, a number of potential in vivo modulators must be considered.

(1) The affinity states of the dopamine D_2 receptor are regulated by guanyl-nucleotide-binding proteins (G proteins) (Wreggett and Seeman, 1983). In general, agonists predominantly label high-affinity state (Sibley et al., 1982; Dubois et al., 1986) and antagonists label both high- and low-affinity state receptors (Sibley et al., 1982; Severson and Randall, 1985). Therefore, the difference in the increase of V_3' in the two regions studied in this study could reflect different proportions of high- and low-affinity state receptors in these regions. In fact, the proportions of these two states varied among regions (Camps et al., 1989). (2) It is generally believed that agonists cause receptor internalization (Dumartin et al., 1998; Ito et al., 1999) and this process affected in vivo binding of dopamine D_2 receptor radioligand (Chugani et al., 1988). All effective neuroreceptor ligands must pass the blood brain barrier, which is essentially composed of a lipophilic membrane. Thus, such tracers should pass the plasma membrane and have access to internalized receptors. However, various radiotracers (e.g., benzamide vs. spirodecanone) may differ in their affinity for the internalized vs. membrane bound receptor. (3) There may be a difference in pharmacodynamic effects of α-methyl-*para*-tyrosine on tyrosine hydroxylase between the thalamus and the temporal cortex. In fact, four isoforms of this enzyme were found in human brain showing different regional distributions (Lewis et al., 1993). (4) A significant number of dopamine D_2 receptors are located extrasynaptically (Yung et al., 1995; Khan et al., 1998) where the concentration of dopamine is lower than in the synapse. Thus, dopamine may occupy a smaller percentage of extrasynaptic receptors compared to those within the synapse. The regional differences in % receptor unmasking induced by α-methyl-*para*-tyrosine may be due to a difference in the proportion of dopamine D_2 receptors within and outside the synapse in the thalamus and cortex (Khan et al., 1998).

In conclusion, this study demonstrated that under equilibrium condition, the binding of a high affinity tracer, [^{123}I]epidepride, was affected by the presence of endogenous dopamine. Furthermore, the increase in dysphoria was correlated with the apparent depletion of dopamine in the temporal cortex. Because extrastriatal dopamine D_2 receptors can be studied with this tracer, endogenous dopamine levels can be estimated by comparing the binding potential at baseline and with dopamine depletion. Although it may be difficult to detect a decreased level of endogenous dopamine in patients, an increased level, as reported in the striatum using [^{123}I]IBZM (Abi-Dargham et al., 1998), will be detected with [^{123}I]epidepride in extrastriatal region. Therefore, this method will be valuable to better understand dopamine activities in extrastriatal regions in schizophrenia and other psychiatric disorders.

Acknowledgements

We thank the technologist staff of the NeuroSPECT laboratory at Yale/Temple Medical Center; Nallakkandi Rajeevan, PhD for nuclear medicine expertise; Louis Amici for radiochemistry procedures; Sylvia Hu, PhD for statistical analysis; Robert W. Reynolds for HVA and MHPG measurements; Haleh Nadim for α-methyl-*para*-tyrosine measurements; Sue Giddings for subject recruitment; Richard Feinn and Quinn Ramsby for image analysis. This work was supported by funds from NIH (MH44866), The Department of Veterans Affairs (VA Schizophrenia Research Center) and NARSAD.

References

Abi-Dargham, A., Gandelman, M., Zoghbi, S.S., Laruelle, M., Baldwin, R.M., Randall, P., Zea-Ponce, Y., Charney, D.S., Hoffer, P.B., Innis, R.B., 1995. Reproducibility of SPECT measurement of benzodiazepine receptors in human brain with [^{123}I]iomazenil. J. Nucl. Med. 36, 167–175.

Abi-Dargham, A., Kegeles, L., Zea-Ponce, Y., Printz, D., Gil, R., Rodenhiser, J., Weiss, R., Schneider, D., Van Heertum, R., Mann, J.J., Gorman, J., Laruelle, M., 1999. Removal of endogenous dopamine reveals elevation of D_2 receptors in schizophrenia. J. Nucl. Med. 40, [Abstract] 30 pp.

Abi-Dargham, A., Printz, D., Kegeles, L., Rodenhiser, J., Zea-Ponce, Y., Weiss, R., Ponzniakoff, T., Gorman, J., Van Heertum, R., Laruelle, M., 1998. SPECT imaging of resting dopamine synaptic release in the striatum of untreated schizophrenic patients. J. Nucl. Med. 39, [Abstract] 82 pp.

Al-Tikriti, M.S., Baldwin, R.M., Zea-Ponce, Y., Sybirska, E., Zoghbi, S.S., Laruelle, M., Malison, R.T., Kung, H.F., Kessler, R.M., Charney, D.S., Hoffer, P.B., Innis, R.B., 1994. Comparison of three high affinity SPECT radiotracers for the dopamine D_2 receptor. Nucl. Med. Biol. 21, 179–188.

Anderson, G.M., Young, J.G., Cohen, D.J., 1979. A rapid liquid chromatographic method for determination of tyrosine, tryptophan, 5-hydroxyindoleacetic acid and homovanillic acid in cerebrospinal fluid. J. Chromatogr. 164, 501–505.

Baldwin, R.M., Zea-Ponce, Y., Zoghbi, S.S., Al-Tikriti, M.S., Seibyl, J.P., Sybirska, E.H., Malison, R.T., Laruelle, M., Charney, D.S., Hoffer, P.B., Innis, R.B., 1994. Pharmacokinetics of the three dopamine D_2 receptor ligands [^{123}I]IBF, [^{123}I]epidepride, and [^{123}I]2′-ISP in nonhuman primates. Nucl. Med. Biol. 21, 969–976.

Breier, A., Su, T.P., Saunders, R., Carson, R.E., Kolachana, B.S., deBartolomeis, A., Weinberger, D.R., Weisenfeld, N., Malhotra, A.K., Eckelman, W.C., Pickar, D., 1997. Schizophrenia is associated with elevated amphetamine-induced synaptic dopamine concentrations: evidence from a novel positron emission tomography method. Proc. Natl. Acad. Sci. U.S.A. 94, 2569–2574.

Camps, M., Cortés, R., Gueye, B., Probst, A., Palacios, J.M., 1989. Dopamine receptors in human brain: autoradiographic distribution of D_2 sites. Neuroscience 28, 275–290.

Chouinard, G., Ross-Chourinard, A., Annable, L., Jones, B.D., 1980. The extrapyramidal symptom rating scale. Can. J. Neurol. Sci. 7, 233.

Chugani, D.C., Ackermann, R.F., Phelps, M.E., 1988. In vivo [^{3}H]spiperone binding: evidence for accumulation in corpus striatum by agonist-mediated receptor internalization. J. Cereb. Blood Flow Metab. 8, 291–303.

Creese, I., Burt, D.R., Snyder, S.H., 1976. Dopamine receptor binding predicts clinical and pharmacological potencies of antischizophrenic drugs. Science 192, 481–483.

Davis, K.L., Kahn, R.S., Ko, G., Davidson, M., 1991. Dopamine in schizophrenia: a review and reconceptualization. Am. J. Psychiatry 148, 1474–1486.

Delforge, J., Bottlaender, M., Loc'h, C., Guenther, I., Fuseau, C., Bendriem, B., Syrota, A., Maziere, B., 1999. Quantitation of extrastriatal D2 receptors using a very high-affinity ligand (FLB 457) and the multi-injection approach. J. Cereb. Blood Flow Metab. 19, 533–546.

Dewey, S.L., Logan, L., Wolf, A.P., Brodie, J.D., Angrist, B., Fowler, J.S., Volkow, N.D., 1991. Amphetamine induced decreases in (18F)-*N*-methylspiroperidol binding in the baboon brain using positron emission tomography (PET). Synapse 7, 324–327.

Dewey, S.L., Smith, G.S., Logan, J., Brodie, J.D., Yu, D.W., Ferrieri, R.A., King, P.T., MacGregor, R.R., Martin, T.P., Wolf, A.P., Volkow, N.D., Fowler, J.S., Meller, E., 1992. GABAergic inhibition of endogenous dopamine release measured in vivo with ^{11}C-raclopride and positron emission tomography. J. Neurosci. 12, 3773–3780.

Dubois, A., Savasta, M., Curet, O., Scatton, B., 1986. Autoradiographic distribution of the D_1 agonist [^{3}H]SKF 38393 in the rat brain and spinal cord. Comparison with the distribution of D_2 dopamine receptors. Neuroscience 19, 125–137.

Dumartin, B., Caillé, I., Gonon, F., Bloch, B., 1998. Internalization of D1 dopamine receptor in striatal neurons in vivo as evidence of activation by dopamine agonists. J. Neurosci. 18, 1650–1661.

Elsworth, J.D., Roth, R.H., Redmond, D.E.J., 1983. Relative importance of 3-methoxy-4-hydroxyphenylglycol and 3,4-dihydroxyphenylglycol as norepinephrine metabolites in rat, monkey, and humans. J. Neurochem. 41, 786–793.

Endres, C.J., Kolachana, B.S., Saunders, R.C., Su, T., Weinberger, D., Breier, A., Eckelman, W., Carson, R.E., 1997. Kinetic modeling of [^{11}C]raclopride: combined PET-microdialysis studies. J. Cereb. Blood Flow Metab. 17, 932–942.

Farde, L., Eriksson, L., Blomquist, G., Halldin, C., 1989. Kinetic analysis of central [^{11}C]-raclopride binding to D_2 dopamine receptors studied with PET — a comparison to the equilibrium analysis. J. Cereb. Blood Flow Metab. 9, 696–708.

Farde, L., Suhara, T., Nyberg, S., Karlsson, P., Nakashima, Y., Hietala, J., Halldin, C., 1997. A PET-study of [^{11}C]FLB 457 binding to extrastriatal D2-dopamine receptors in healthy subjects and antipsychotic drug-treated patients. Psychopharmacology 133, 396–404.

Friston, K.J., Ashburner, J., Poline, J.B., Frith, C.D., Heather, J.D., Frackowiak, R.S.J., 1995. Spatial registration and normalisation of images. Human Brain Mapping 2, 165–189.

Fujita, M., Seibyl, J.P., Verhoeff, N.P.L.G., Ichise, M., Baldwin, R.M., Zoghbi, S.S., Burger, C., Staley, J.K., Rajeevan, N., Charney, D.S., Innis, R.B., 1999. Kinetic and equilibrium analyses of [^{123}I]epidepride binding to striatal and extrastriatal dopamine D_2 receptors. Synapse 34, 290–304.

Ginovart, N., Farde, L., Halldin, C., Swahn, C.G., 1997. Effect of reserpine-induced depletion of synaptic dopamine on [11C]raclopride binding to D2-dopamine receptors in the monkey brain. Synapse 25, 321–325.

Grace, A.A., 1993. Cortical regulation of subcortical systems and its possible relevance to schizophrenia. J. Neural Transm. [Gen. Sect.] 91, 111–134.

Hall, H., Farde, L., Halldin, C., Hurd, Y.L., Pauli, S., Sedvall, G., 1996. Autoradiographic localization of extrastriatal D2-dopamine receptors in the human brain using [^{125}I]epidepride. Synapse 23, 115–123.

Ichise, M., Fujita, M., Seibyl, J.P., Verhoeff, N.P., Baldwin, R.M., Zoghbi, S.S., Rajeevan, N., Charney, D.S., Innis, R.B., 1999. Graphical modeling and simplified quantification of striatal and extrastriatal dopamine D2 receptor binding with iodine-123-epidepride SPECT. J. Nucl. Med. 40, 1902–1912.

Iida, H., Narita, Y., Kado, H., Kashikura, A., Sugawara, S., Shoji, Y., Kinoshita, T., Ogawa, T., Eberl, S., 1998. Effects of scatter and attenuation correction on quantitative assessment of regional cerebral blood flow with SPECT. J. Nucl. Med. 39, 181–189.

Innis, R.B., Malison, R.T., Al-Tikriti, M., Hoffer, P.B., Sybirska, E.H., Seibyl, J.P., Zoghbi, S.S., Baldwin, R.M., Laruelle, M.A., Smith, E., Charney, D.S., Heninger, G., Elsworth, J.D., Roth, R.H., 1992. Amphetamine-stimulated dopamine release competes in vivo for [^{123}I]IBZM binding to the D2 receptor in nonhuman primates. Synapse 10, 177–184.

Ito, H., Hietala, J., Blomqvist, G., Halldin, C., Farde, L., 1998. Comparison of the transient equilibrium and continuous infusion method for quantitative PET analysis of [^{11}C]raclopride binding. J. Cereb. Blood Flow Metab. 18, 941–950.

Ito, K., Haga, T., Lameh, J., Sadee, W., 1999. Sequestration of dopamine D2 receptors depends on coexpression of G-protein-coupled receptor kinases 2 or 5. Eur. J. Biochem. 260, 112–119.

Kessler, R.M., Mason, N.S., Votaw, J.R., Depaulis, T., Clanton, J.A., Ansari, M.S., Schmidt, D.E., Manning, R.G., Bell, R.L., 1992. Visualization of extrastriatal dopamine D2 receptors in the human brain. Eur. J. Pharmacol. 223, 105–107.

Kessler, R.M., Votaw, J.R., Schmidt, D.E., Ansari, M.S., Holdeman, K.P., de Paulis, T., Clanton, J.A., Pfeffer, R., Manning, R.G., Ebert, M.H., 1993. High affinity dopamine D2 receptor radioligands. 3. [^{123}I] and [^{125}I]epidepride: in vivo studies in rhesus monkey brain and comparison with in vitro pharmacokinetics in rat brain. Life Sci. 53, 241–250.

Khan, Z.U., Gutierrez, A., Martin, R., Penafiel, A., Rivera, A., De La Calle, A., 1998. Differential regional and cellular distribution of dopamine D2-like receptors: an immunocytochemical study of subtype-specific antibodies in rat and human brain. J. Comp. Neurol. 402, 353–371.

Laruelle, M., Abi-Dargham, A., van Dyck, C.H., Gil, R., D'Souza, C.D., Erdos, J., McKance-Katz, E., Rosenblatt, W., Fingado, C., Zoghbi, S.S., Baldwin, R.M., Seibyl, J.P., Krystal, J., Charney, D.S., Innis, R.B., 1996. SPECT imaging of amphetamine-induced dopamine release in drug free schizophrenic subjects. Proc. Natl. Acad. Sci. U.S.A. 93, 9235–9240.

Laruelle, M., D'Souza, C., Baldwin, R.M., Abi-Dargham, A., Kanesm, S., Fingado, C.L., Seibyl, J.P., Bowers, M.B., Charney, D.S., Innis, R.B., 1997. Imaging D2 receptor occupancy by endogenous dopamine in humans. Neuropsychopharmacology 17, 162–174.

Lewis, D.A., Melchitzky, D.S., Haycock, J.W., 1993. Four isoforms of tyrosine hydroxylase are expressed in human brain. Neuroscience 54, 477–492.

Mukherjee, J., Yang, Z.Y., Das, M.K., Brown, T., 1995. Fluorinated benzamide neuroleptics. III. Development of (*S*)-*N*-[(1-allyl-2-pyrrolidinyl)methyl]-5-(3-[^{18}F]fluoropropyl)-2,3-dimethoxybenzamide as an improved dopamine D-2 receptor tracer. Nucl. Med. Biol. 22, 283–296.

Narang, N., Wamsley, J.K., 1995. Time dependent changes in DA uptake sites, D1 and D2 receptor binding and mRNA after 6-OHDA lesions of the medial forebrain bundle in the rat brain. J. Chem. Neuroanat. 9, 41–53.

Rajeevan, N., Zubal, I.G., Ramsby, S.Q., Zoghbi, S.S., Seibyl, J., Innis, R.B., 1998. Significance of nonuniform attenuation correction in quantitative brain SPECT imaging. J. Nucl. Med. 39, 1719–1726.

Reynolds, G.P., 1989. Beyond the dopamine hypothesis, the neurochemical pathology of schizophrenia. Br. J. Psychiatry 155, 305–316.

Rieck, R.W., Ansari, M.S., Mason, N.S., Whetsell, W.O., Kessler, R.M., 1997. Selective distribution of dopamine D2 and D3 receptors sub-

types within the human thalamus defined with in vivo PET imaging and receptor autoradiography in postmortem tissue. J. Nucl. Med. 38, [Abstract] 81 pp.

Ross, S., Jackson, D.M., 1989. Kinetic properties of the accumulation of ^{3}H-raclopride in the mouse brain in vivo. Naunyn-Schiedeberg's Arch. Pharmacol. 340, 6–12.

Seeman, P., Lee, T., 1975. Antisychotic drugs: direct correlation between clinical potency and presynaptic action on dopamine neurons. Science 188, 1217–1219.

Seeman, P., Guan, H.-C., Niznik, H.B., 1989. Endogenous dopamine lowers the dopamine D2 receptor density as measured by [^{3}H]raclopride: Implications for positron emission tomography of the human brain. Synapse 3, 96–97.

Severson, J.A., Randall, P.K., 1985. D2 dopamine receptors in aging mouse striatum: determination of high and low affinity agonist binding sites. J. Pharmacol. Exp. Ther. 233, 361–368.

Sibley, D.R., De Lean, A., Creese, I., 1982. Anterior pituitary dopamine receptors. Demonstration of interconvertible high and low affinity states of the D_2 dopamine receptor. J. Biol. Chem. 257, 6351–6361.

Varrone, A., Fujita, M., Verhoeff, N.P.L.G., Zoghbi, S.S., Baldwin, R.M., Rajeevan, N., Charney, D.S., Seibyl, J.P., Innis, R.B., in press. Test-retest reproducibility of extrastriatal dopamien D2 receptor imaging with [^{123}I]epidepride SPECT in humans. J. Nucl. Med.

Volkow, N.D., Wang, G.J., Fowler, J.S., Logan, J., Schlyer, D., Hitzemann, R., Lieberman, J., Angrist, B., Pappas, N., Burr, G., Cooper, T., Wolf, A.P., 1994. Imaging endogenous dopamine competition with [^{11}C]raclopride in the human brain. Synapse 16, 255–262.

Weinberger, D.R., 1987. Implications of normal brain development for the pathogenesis of schizophrenia. Arch. Gen. Psychiatry 44, 660–669.

White, L., Harvey, P.D., Opler, L., Lindenmayer, J.P., 1997. Empirical assessment of the factorial structure of clinical symptoms in schizophrenia. A multisite, multimodel evaluation of the factorial structure of the Positive and Negative Syndrome Scale. The PANSS Study Group. Psychopathology 30, 263–274.

Woods, R.P., Mazziotta, J.C., Cherry, S.R., 1993. MRI-PET registration with automated algorithm. J. Comp. Assist. Tomogr. 17, 536–546.

Wreggett, K.A., Seeman, P., 1983. Agonist high and low affinity states of the D2 dopamine receptor in calf brain. Mol. Pharmacol. 25, 10–17.

Yung, K.K., Bolam, J.P., Smith, A.D., Hersch, S.M., Ciliax, B.J., Levey, A.I., 1995. Immunocytochemical localization of D1 and D2 dopamine receptors in the basal ganglia of the rat: light and electron microscopy. Neuroscience 65, 709–730.

Zoghbi, S.S., Baldwin, R.M., Seibyl, J.P., Al-Tikriti, M.S., Zea-Ponce, Y., Laruelle, M., Sybirska, E.H., Woods, S.W., Goddard, A.W., Charney, D.S., Smith, E.O., Hoffer, P.B., Innis, R.B., 1992. Pharmacokinetics of the SPECT benzodiazepine receptor radioligand [^{123}I]iomazenil in human and nonhuman primates. Nucl. Med. Biol. - Int. J. Rad. App. B 19, 881–888.